2942 *Inorg. Chem.* **1991**, *30*, 2942-2949

Contribution from the Department of Chemistry,
The University of North Carolina at Chapel Hill, Chapel Hill, North Carolina 27599-3290

Formation of Thin Polymeric Films by Electropolymerization. Reduction of Metal Complexes Containing Bromomethyl-Substituted Derivatives of 2,2'-Bipyridine

Sharon Gould, Geoffrey F. Strouse, Thomas J. Meyer,* and B. Patrick Sullivan*,†

Received December 28, 1990

Polypyridyl complexes of Fe^{II} and Ru^{II} containing the ligands 4,4'-bis(bromomethyl)-2,2'-bipyridine or 4-(bromomethyl)-4'-methyl-2,2'-bipyridine have been prepared. Upon electrochemical reduction of the complexes, coupling reactions occur at the ligands that yield thin, metal-complex containing, polymeric films on electrode surfaces. The coupling reaction was also found to occur for the free ligand to give an electrode coated with a thin, poly(bipyridine) film. When exposed to a solution containing $FeCl_2$, these films incorporated Fe^{II} by forming a tris(bipyridyl) complex. The rates of electropolymerization of the complexes have been studied relative to complexes containing the polymerizable ligand 4-methyl-4'-vinyl-2,2'-bipyridine (vbpy). Films prepared by the electrochemical polymerization of the bromomethyl-substituted, bipyridine-containing complexes appear to be less dense and more permeable than films obtained by electrochemical polymerization of analogous complexes containing the vbpy ligand. Copolymeric films, in which more than one complex is incorporated into a single layer, have been prepared as have "bilayer" films, in which different complexes are spatially separated in separate layers.

Introduction

Metal complexes have been prepared which upon oxidation or reduction undergo electropolymerization to form thin polymeric films on electrodes. Electrochemical reduction of complexes containing vinylic or acetylenic substituents on bipyridine ligands or oxidation of aromatic amines leads to polymerization.[1-4] Although this chemistry is extensive, it is not encyclopedic. There is a continuing need to identify new reactions and new molecules that can lead to the formation of stable films.

Electropolymerization techniques have been applied to the preparation of films by reduction of metal-macrocyclic complexes that contain dihalobenzyl substituents[5a] and metal-polypyridyl complexes that contain chloro substituents.[5b] In this paper, we extend that chemistry and show that the ligands 4-(bromomethyl)-4'-methyl-2,2'-bipyridine (4-CH_2Br-4'-CH_3bpy) and 4,4'-bis(bromomethyl)-2,2'-bipyridine (4,4'-$(CH_2Br)_2$bpy) and their complexes undergo facile, reductive electropolymerization to give stable, polymeric films on electrodes.

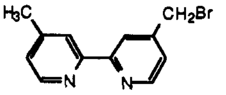

4-CH_2Br-4'-CH_3bpy

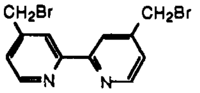

4,4'-$(CH_2Br)_2$bpy

Experimental Section

Materials. The ligand 4,4'-dimethyl-2,2'-bipyridine (Aldrich) was recrystallized from ethyl acetate. The initiators *N*-bromosuccinimide (NBS) (Aldrich) and azobis(isobutyronitrile) (AIBN) (Kodak) were purified by literature methods.[6] The complex *cis*-$Ru(bpy)_2Cl_2 \cdot 2H_2O$ (bpy is 2,2'-bipyridine) was prepared by literature methods.[7] Ammonium hexafluorophosphate (Aldrich), tetraethylammonium hexafluorophosphate (GFS Chemical Co.), ammonium iron(II) sulfate (Allied Chemical Co.), and zinc chloride (Allied Chemical Co.) were used as received. Tetra-*n*-butylammonium hexafluorophosphate was precipitated from water by adding hexafluorophosphoric acid (Aldrich) to an aqueous solution of tetra-*n*-butylammonium bromide (Aldrich). The precipitate was recrystallized twice from ethanol, dissolved in a minimum amount of CH_2Cl_2, and precipitated by the addition of diethyl ether. All solvents were reagent grade and used as supplied except where noted. Spectrophotometric grade acetonitrile (Burdick and Jackson) was used for all electrochemical and spectrophotometric measurements.

Measurements. ^1H NMR spectral data for the ligands and their complexes were recorded in either $CDCl_3$ or CD_3CN with a Bruker AC200 spectrometer. Spectrophotometric measurements in the visible were recorded in either CH_3CN or CH_2Cl_2 with a Hewlett Packard 8451A diode-array spectrophotometer using 1-cm quartz cells.

Electrochemistry. Cyclic voltammetric experiments were carried out by using a Princeton Applied Research Model 174A polarographic analyzer, a home-built waveform generator, and a Hewlett Packard 7015B X-Y recorder. All potentials were recorded relative to the Ag/0.01 M $AgNO_3$[8] reference electrode unless otherwise noted.

Rotated disk experiments were performed by using a Pine Instruments Co. Model RDE4 potentiostat and a Pine Instruments Co. Model ASR and ASRP speed control/rotator assembly. The experiments were carried out in a one-compartment cell by using ca. 0.13-cm^2 Teflon-shrouded Pt disk working electrodes and a saturated sodium calomel (SSCE) reference electrode. They were conducted in acetonitrile solutions, which were 0.1 M in $[NEt_4](ClO_4)$ and 0.068-0.136 mM in the electroactive species. Voltammograms were measured at a range of rotation rates from 200 to 4500 rpm in a cell exposed to the atmosphere. In control experiments at an uncoated electrode, plots of i_{lim} vs $\omega^{1/2}$ were linear with an intercept that was close to zero, consistent with limiting Levich behavior.

Preparations. 4-(Bromomethyl)-4'-methyl-2,2'-bipyridine (4-CH_2Br-4'-CH_3bpy).[9] This compound was prepared by a variation of a published procedure.[10] The compounds 4,4'-dimethyl-2,2'-bipyridine (1.8 g, 9.68 mmol), *N*-bromosuccinimide (1.8 g, 10.1 mmol), and azobis(isobutyronitrile) (0.05 g) were added to CCl_4 (40 mL). The resulting solution was heated at reflux under Ar for 2 h. The mixture was cooled to room temperature, filtered, and evaporated to near dryness. The residue was redissolved in CH_2Cl_2 and purified by column chromatography on silica

---

* To whom correspondence should be addressed.

† Current address: Department of Chemistry, University of Wyoming, Laromie, WY 82071.

(1) (a) Denisevich, P.; Abruña, H. D.; Leidner, C. R.; Meyer, T. J.; Murray, R. W. *Inorg. Chem.* **1982**, *21*, 2153. (b) Abruña, H. D.; Denisevich, P.; Umana, M.; Meyer, T. J.; Murray, R. W. *J. Am. Chem. Soc.* **1981**, *103*, 1. (c) Calvert, J. M.; Peebles, D. L.; Nowak, R. J. *Inorg. Chem.* **1985**, *24*, 3111. (d) Potts, K. T.; Usifer, D.; Guadalupe, A.; Abruña, H. D. *J. Am. Chem. Soc.* **1987**, *109*, 3961. (e) Meyer, T. J.; Sullivan, B. P.; Caspar, J. V. *Inorg. Chem.* **1987**, *26*, 4145. (f) Leidner, C. R.; Sullivan, B. P.; Reed, R. A.; White, B. A.; Crimmins, M. T.; Murray, R. W.; Meyer, T. J. *Inorg. Chem.* **1987**, *26*, 882. (g) Calvert, J. M.; Schmehl, R. H.; Sullivan, B. P.; Facci, J. S.; Meyer, T. J.; Murray, R. W. *Inorg. Chem.* **1983**, *22*, 2151. (h) Calvert, J. M.; Sullivan, B. P.; Meyer, T. J. In *Chemically Modified Surfaces in Catalysis and Electrocatalysis*; Miller, J., Ed.; ACS Symposium Series 192; American Chemical Society: Washington, DC, 1982; p 159. (i) Abruña, H. D.; Calvert, J. M.; Denisevich, P.; Ellis, C. D.; Meyer, T. J.; Murphy, W. R.; Murray, R. W.; Sullivan, B. P.; Walsh, J. L. In *Chemically Modified Surfaces in Catalysis and Electrocatalysis*; Miller, J., Ed.; ACS Symposium Series 192; American Chemical Society: Washington, DC, 1982; p 133.

(2) (a) Hoferkamp, L. A.; Goldsby, K. A. *Chem. Mater.* **1989**, *1*, 348. (b) Ellis, C. D.; Margerum, L. D.; Murray, R. W.; Meyer, T. J. *Inorg. Chem.* **1983**, *22*, 1283.

(3) (a) White, B. A.; Murray, R. W. *J. Electroanal. Chem. Interfacial Electrochem.* **1985**, *189*, 345. (b) Spiro, T. G.; Macor, K. A. *J. Am. Chem. Soc.* **1983**, *105*, 5601. (c) Kellet, R. M.; Spiro, T. G. *Inorg. Chem.* **1985**, *24*, 2378.

(4) Abruña, H. D. *Coord. Chem. Rev.* **1988**, *86*, 135.

(5) (a) Fussa-Rydel, O.; Zhang, H.-T.; Hupp, J. T.; Leidner, C. R. *Inorg. Chem.* **1989**, *28*, 1553. (b) Deronizer, A.; Marques, M.-J. *J. Electroanal. Chem. Interfacial Electrochem.* **1989**, *265*, 341.

(6) Perrin, D. D.; Armarego, W. L. F.; Perrin, D. R. *Purification of Laboratory Chemicals*, 2nd ed.; Pergamon: Oxford, England, 1980.

(7) Sullivan, B. P.; Salmon, D. J.; Meyer, T. J. *Inorg. Chem.* **1978**, *17*, 3334.

(8) The Ag/$AgNO_3$ reference electrode was 0.01 M $AgNO_3$ in 0.1 M $[N(Et)_4](ClO_4)$/acetonitrile. The potential of the electrode is +0.3 V vs SSCE.

(9) Boyde, S.; Strouse, G. F.; Jones, W.; Meyer, T. J. Manuscript in preparation.

(10) Eaves, J. G.; Munro, H. S.; Parker, D. K. *Inorg. Chem.* **1987**, *26*, 644.

(Aldrich 230–400 mesh) by eluting with 98:2 (v/v) CH_2Cl_2/acetone. The product eluted as the second band. The fractions containing the pure product were combined and evaporated to dryness to give 0.75 g (30% yield) of an oily white solid. ^1H NMR (δ (ppm), $CDCl_3$): 2.45 (s, 3 H), 4.46 (s, 2 H), 7.16 (unresolved dd, 5.0 Hz, 1 H), 7.33 (dd, 5 Hz, 1.8 Hz, 1 H), 8.23 (1 H, unresolved d), 8.42 (unresolved d, 1 H), 8.53 (d, 5.0 Hz, 1 H), 8.64 (d, 4.9 Hz, 1 H).

4,4′-Bis(bromomethyl)-2,2′-bipyridine (4,4′-$(CH_2Br)_2$bpy). This compound was prepared by a procedure analogous to the one used for 4-CH_2Br-4′-CH_3bpy. To a mixture of 4,4′-dimethyl-2,2′-bipyridine (8.00 g, 43.5 mmol) and *N*-bromosuccinimide (16 g, 89.89 mmol) in 300 mL of refluxing CCl_4 (distilled from P_2O_5) was added azobis(butyronitrile) (500 mg). The resulting solution was allowed to stir for 3 h under Ar, cooled in an ice bath, filtered to remove precipitated succinimide, and evaporated to dryness by using a rotary evaporator. The residue was dissolved in a minimum of CH_2Cl_2 and purified by column chromatography on silica (Aldrich 230–400 mesh) by eluting with 98:2 (v/v) CH_2Cl_2/acetone. The product eluted as the first band. After collection, the solvent was evaporated to near dryness and the product was collected as a pure white precipitate by the addition of hexane (yield: 4.46 g, 30%). ^1H NMR (δ (ppm), $CDCl_3$): 4.47 (s, 4 H), 7.35 (dd, 1 Hz, 5 Hz, 2 H), 8.42 (d, 1 Hz, 2 H), 8.65 (d, 5 Hz, 2 H).

$[Fe^{II}(L)_3](PF_6)_2$ (L = 4-CH_2Br-4′-CH_3bpy, 4,4′-$(CH_2Br)_2$bpy). To a stirred solution of CH_3OH (20 mL) was added 0.100 g of $Fe(NH_4)_2(SO_4)_2 \cdot 6H_2O$ (0.255 mmol) and 0.201 g of 4-CH_2Br-4′-CH_3bpy (0.765 mmol). The solution turned red immediately. It was stirred for 1 h under Ar, at which point the complex was precipitated from CH_3OH as the PF_6^- salt by the addition of NH_4PF_6 (saturated in H_2O). After filtration, the complex was reprecipitated from CH_2Cl_2 by the addition of anhydrous diethyl ether (yield: 0.256 g, 89%). Anal. Calcd for $C_{36}H_{33}N_6Br_3FeP_2F_{12}$: C, 38.06; H, 2.90; N, 7.40. Found: C, 38.06; H, 3.22; N, 7.20. ^1H NMR (δ (ppm), $CDCl_3$): 2.53 (s, 3 H), 4.65 (s, 2 H), 7.29 (m, 4 H); 8.41 (s, 1 H), 8.53 (s, 1 H). UV/vis (λ_{max} (nm), CH_3CN): 302 (58500 M^{-1} cm^{-1}), 360 (7400), 532 (9700).

The preparation and purification of $[Fe^{II}(4,4'\text{-}(CH_2Br)_2bpy)_3](PF_6)_2$ was carried out in similar fashion by using 0.050 g of 4,4′-$(CH_2Br)_2$bpy (0.190 mol) and 0.025 g of $Fe(NH_4)_2(SO_4)_2 \cdot 6H_2O$ (0.064 mol) in 20 mL of CH_3OH for 1 h under Ar (0.08 g, 90%). Anal. Calcd for $C_{36}H_{30}N_6Br_6FeP_2F_{12}$: C, 31.5; H, 2.2; N, 6.12. Found: C, 31.11; H, 1.94; N, 5.91. ^1H NMR (δ (ppm), CD_3CN): 4.65 (s, 4 H), 7.31 (d, 4.8 Hz, 2 H), 7.42 (unresolved d, 2 H), 8.56 (s, 2 H). UV/vis (λ_{max} (nm), CH_3CN): 308 (60 100 M^{-1} cm^{-1}), 370 (11 500), 536 (13 600).

$[Zn^{II}(4\text{-}CH_2Br\text{-}4'\text{-}CH_3bpy)_3](PF_6)_2$. To a stirred solution of CH_3OH was added $ZnCl_2$ (0.011 g, 0.083 mol) and 4-CH_2Br-4′-CH_3bpy (0.066 g, 0.250 mol). After the mixture was stirred under Ar for 3 h, addition of a saturated solution of NH_4PF_6 in CH_3OH caused immediate precipitation of the desired product. The salt was reprecipitated by the addition of anhydrous diethyl ether to a CH_2Cl_2 solution. Anal. Calcd for $C_{36}H_{33}N_6Br_3ZnP_2F_{12}$: C, 35.0; H, 3.17; N, 8.0; Br, 23.1. Found: C, 37.0; H, 3.01; N, 7.22; Br, 19.0. ^1H NMR (δ (ppm), $CDCl_3$): 2.52 (s, 3 H), 4.62 (s, 2 H), 7.39 (s, 1 H), 7.55 (s, 1 H), 7.73 (s, 1 H), 7.83 (s, 1 H), 8.35 (s, 1 H), 8.49 (s, 1 H). UV/vis is (λ_{max} (nm), CH_2Cl_2): 300 (41 200 M^{-1} cm^{-1}), 244 (34 900), 208 (97 200).

$[Ru^{II}(bpy)_2(4,4'\text{-}(CH_2Br)_2bpy)](PF_6)_2$. The compound *cis*-Ru$(bpy)_2Cl_2 \cdot 2H_2O$ (0.1069 g, 0.202 mmol) and silver triflate (0.107 g, 0.416 mmol) were combined in 9 mL of acetone (distilled from K_2CO_3) and allowed to stir for 8 h under N_2. The precipitated AgCl was removed by filtration. To the filtrate, which contained $[Ru(bpy)_2(acetone)_2]^{2+}$, was added directly 4,4′-$(CH_2Br)_2$bpy (0.0692 g, 0.200 mmol). After stirring for 2 h, the red solution was evaporated to dryness. The product was dissolved in H_2O, precipitated by the addition of aqueous NH_4PF_6, and purified by column chromatography on an alumina column with toluene/acetonitrile (1:1) as the eluent. After drying, the desired product was reprecipitated from CH_2Cl_2 by dropwise addition of diethyl ether. Anal. Calcd for $C_{32}H_{26}N_6Br_2RuP_2F_{12}$: C, 36.77; H, 2.49; N, 8.04. Found: C, 36.09; H, 2.38; N, 7.79. ^1H NMR (δ (ppm), CD_3CN): 4.66 (s, 4 H), 7.40 (m, 6 H), 7.69 (m, 6 H), 8.09 (m, 6 H), 8.50 (m, 6 H). UV/vis (λ_{max} (nm), CH_3CN): 456 (12 200 M^{-1} cm^{-1}), 290 (60 900), 246 (23 500).

Preparation of the Films. Electropolymerization of the complexes was accomplished in a one-compartment cell by using monomer concentrations of 0.02–2.0 mM in acetonitrile solutions containing 0.1 M $[N(n\text{-}Bu)_4](PF_6)$. Polymeric films were grown by cycling the potential of the working electrode either between 0 and −2.0 V or between +1.4 and −2.0 V. All experiments were carried out under a N_2 atmosphere in a Vacuum Atmospheres glovebox that had been modified to operate under a constant N_2 purge.

All films were prepared by using ca. 0.13–cm^2, Teflon-shrouded Pt disk working electrodes except those used for film density, X-ray photoelectron spectroscopic (XPS), or UV/vis spectrophotometric measurements. Disk electrodes were polished by using 1.0-μm diamond paste (Buehler) and rinsed well with H_2O and acetone prior to use. Silicon wafers that had been coated with ~1000 Å of Pt (NTT of Japan) were used as the conductive substrate for the film density and XPS measurements. Transparent indium tin oxide (ITO) electrodes (Delta Technologies, Limited) were used for the spectrophotometric measurements.

The effective surface coverage, Γ, in mol/cm^2, of a film on an electrode was estimated by measuring the charge associated with the $Fe^{III/II}$ or $Ru^{III/II}$ oxidations by using either planimetry or triangulation to measure the area of the wave in the recorded cyclic voltammogram. Film thickness measurements were carried out by using a Alpha Step 100 profilometer.

Results and Discussion

One aspect of our research effort has been the development of new procedures for preparing thin polymeric films in which the starting monomers are metal complexes. The approach taken here was to exploit the electrochemical reduction of halocarbons where, by radical–radical coupling following halide loss or, perhaps, by displacement of halide by a carbanion, C–C bond formation can occur. In complexes where there are at least two polymerizable sites a basis exists for the formation of a polymeric network following electrochemical reduction. This approach is especially appropriate for ligands containing benzylic-type halide groups, since they are reduced at relatively low potentials.

Preparations and Properties of the Complexes. The ligands 4-CH_2Br-4′-CH_3bpy and 4,4′-$(CH_2Br)_2$bpy were prepared by partial oxidation of the methyl group(s) of 4,4′-dimethyl-2,2′-bipyridine by NBS. The yields were relatively low because of the lack of selectivity that is an inherent property of the radical reactions. A complication in the preparation and handling of the ligands arose from their thermal instability. The instability is presumably due to the formation of cationic, oligomeric pyridiniums that form by the nucleophilic displacement of bromide from the C–Br bond by the pyridine nitrogen atom. The purified ligands were stable for several months without decomposition if stored dry at <0 °C.

Once formed, the complexes show no sign of decomposition in the solid state over several months. The salts $[Fe(L)_3](PF_6)_2$ and $[Zn(L)_3(PF_6)_2$ (L = 4-CH_2Br-4′-CH_3bpy, 4,4′-$(CH_2Br)_2$bpy) were formed in near quantitative yields simply by stirring the appropriate Zn^{II} or Fe^{II} salt in CH_3OH with the free ligand. Isolation and purification was achieved by metathesis to give the PF_6^- salt, collection of the solid by filtration, and reprecipitation from CH_2Cl_2 by the addition of diethyl ether.

In the preparation of $[Ru(bpy)_2(4,4'\text{-}(CH_2Br)_2bpy)](PF_6)_2$, $[Ru(bpy)_2(acetone)_2]^{2+}$ was utilized as an intermediate. It was generated in situ by a published procedure.[7] The reaction was conducted under a N_2 atmosphere without heating in order to minimize self-quaternization by the ligand. Purification by column chromatography on alumina with toluene/CH_3CN was required to purify the complex.

Film Growth. Electrochemical Properties of the Complexes in the Films. In Figure 1A are shown a series of cyclic voltammograms that were recorded during the reductive electropolymerization of $[Fe(4\text{-}CH_2Br\text{-}4'\text{-}CH_3bpy)_3]^{2+}$ at a Pt-disk electrode in 0.1 M $[N(n\text{-}Bu)_4](PF_6)/CH_3CN$ solution. In the initial reductive scan a broad, irreversible reduction appears. It begins at −0.7 V and consists of a number of poorly resolved peaks followed by reversible couples at −1.74 and −1.90 V. On subsequent scans, the irreversible peak sharpens and shifts to more negative potentials and the peak currents for the reversible couples steadily increase in magnitude as increasing amounts of electroactive material are deposited on the electrode surface. Visual inspection of the electrodes following a series of scans revealed the presence of a metallopolymeric film coating that was pink to red depending on film thickness.

During the electropolymerization procedure, the peak potentials in the oxidative branch of the voltammogram changed. Before electropolymerization, a reversible wave for the $Fe^{III/II}$ couple of the monomeric complex appeared at +0.71 V. After polymerization was initiated by a reductive scan, the potential for the $Fe^{III/II}$ couple had shifted to +0.68 V. The shift in potential is consistent

Table I. Electrochemical Data in 0.1 M $[N(n\text{-}Bu)_4](PF_6)$/Acetonitrile vs Ag/0.01 M $AgNO_3$[a]

complex	$E_{1/2}$(oxidn) $M^{III/II}$	$E_{1/2}$(redn) bpy$^{0/-}$	$E_{1/2}$(redn) (bpy$^{0/-}$)$_2$
$[Fe(vbpy)_3]^{2+}$[b]	+0.65		
polymerized $[Fe(vbpy)_3]^{2+}$	+0.69	−1.68	−1.88
$[Fe(4\text{-}CH_2Br\text{-}4'\text{-}CH_3bpy)_3]^{2+}$	+0.71		
polymerized $[Fe(4\text{-}CH_2Br\text{-}4'\text{-}CH_3bpy)_3]^{2+}$	+0.68	−1.69	−1.88
$[Fe(4,4'\text{-}(CH_2Br)_2bpy)_3]^{2+}$	+0.81		
polymerized $[Fe(4,4'\text{-}(CH_2Br)_2bpy)_3]^{2+}$	+0.72	−1.68	−1.87
polymerized $[Zn(4\text{-}CH_2Br\text{-}4'\text{-}CH_3bpy)_3]^{2+}$		−1.75[c]	−1.89[c]
$[Ru(bpy)_2(4,4'\text{-}(CH_2Br)_2bpy)]^{2+}$	+1.00		
polymerized $[Ru(bpy)_2(4,4'\text{-}(CH_2Br)_2bpy)]^{2+}$	+0.97	−1.64	−1.81

[a] The scan rate was 50 mV/s. [b] vbpy is 4-methyl-4'-vinyl-2,2'-bipyridine. [c] The ligand-based reductions for polymerized $[Zn(4\text{-}BrCH_2\text{-}4'\text{-}CH_3bpy)_3]^{2+}$ were frequently observed as a single, broad wave centered at ~−1.85 V.

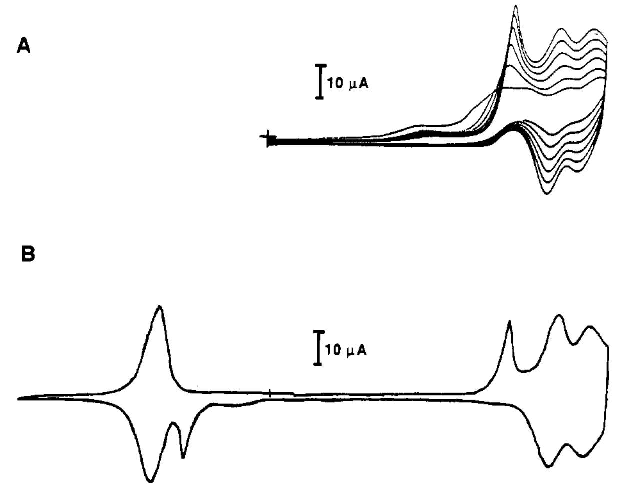

Figure 1. (A) Repetitive cyclic voltammograms of a solution 0.6 mM in $[Fe(4\text{-}CH_2Br\text{-}4'\text{-}CH_3bpy)_3]^{2+}$ in acetonitrile that was 0.1 M in $[N(n\text{-}Bu)_4](PF_6)$ at a Pt-disk electrode of surface area 0.12 cm^2. (B) Cyclic voltammogram of the polymerized $[Fe(4\text{-}CH_2Br\text{-}4'\text{-}CH_3bpy)_3]^{2+}$ film that resulted from (A) in a fresh electrolyte solution. $\Gamma = 7.4 \times 10^{-9}$ mol/cm^2. Scan rate = 50 mV/s.

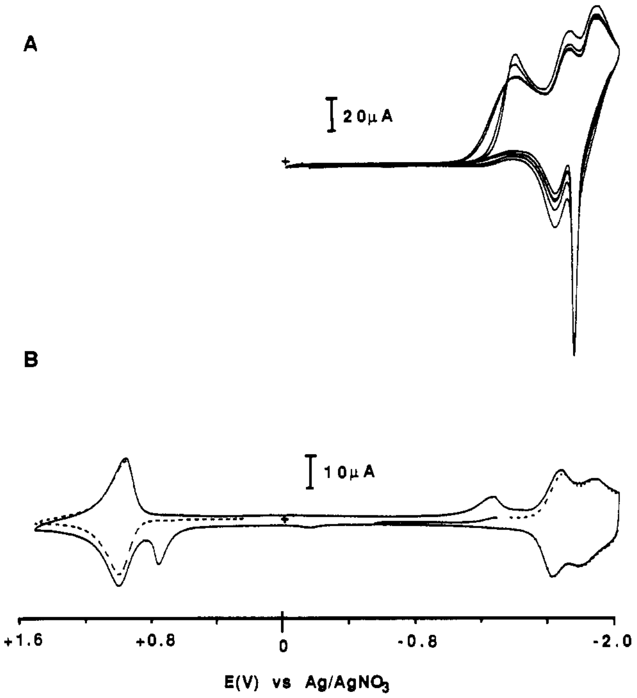

Figure 2. (A) Cyclic voltammograms of a solution 1.39 mM in $[Ru(bpy)_2(4,4'\text{-}(CH_2Br)_2bpy)]^{2+}$, as in Figure 1. The voltammograms are not consecutive but were recorded at various intervals over ~25 min. (B) Cyclic voltammogram of the polymerized $[Ru(bpy)_2(4,4'\text{-}(CH_2Br)_2bpy)_3]^{2+}$ film that resulted from (A), as in Figure 1. The dotted line indicates the voltammetric response when cycling was limited to the oxidative or reductive couples. $\Gamma = 3.0 \times 10^{-9}$ mol/cm^2. Scan rate = 100 mV/s.

with the replacement of an electronegative $BrCH_2$– substituent by a more electron-rich C–C bond that links bipyridine ligands; see below. X-ray photoelectron spectroscopic (XPS) measurements failed to provide evidence for Br^- in the polymerized $[Fe(4\text{-}CH_2Br\text{-}4'\text{-}CH_3bpy)_3]^{2+}$ or $[Fe(4,4'\text{-}(CH_2Br)_2bpy)_3]^{2+}$ films. From these observations we conclude that Br^- is completely lost during the polymerization.

The electrochemistry observed in the films (Figure 1B) is that expected for a confined, polypyridyl complex of Fe^{II}.[1a,b] An $Fe^{III/II}$ oxidation at +0.68 V and two, reversible, ligand-based reductions at −1.69 and −1.88 V appear in the voltammogram. The sharp prepeaks, which are present at the onset of both the $Fe^{III/II}$ oxidation wave and the first ligand reduction wave, disappear if cycling is restricted to either the metal-based oxidation or ligand-based reduction. The appearance of prepeaks of this type has been noted previously in related films.[1a]

The electrochemical behavior of $[Fe(4,4'\text{-}(CH_2Br)_2bpy)_3]^{2+}$ during electropolymerization was similar to that of $[Fe(4\text{-}CH_2Br\text{-}4'\text{-}CH_3bpy)_3]^{2+}$. Cyclic voltammograms of films prepared from the two complexes were essentially identical, but a marked difference in the stabilities of the films was observed. Films of electropolymerized $[Fe(4,4'\text{-}(CH_2Br)_2bpy)_3]^{2+}$ were stable toward multiple scan cycling between +1.4 and −2.0 V. For films prepared from $[Fe(4\text{-}CH_2Br\text{-}4'\text{-}CH_3bpy)_3]^{2+}$, 10 scans in the same potential range resulted typically in the loss of ~30% of the film, as judged by integrated peak current measurements. The instability arose during the reductive part of the scans. No loss was observed if the potential range was confined to 0 to +1.5 V. Instability following reduction has been found previously for other redox polymers of this type.[1a,11] One possible explanation is that reduction decreases the net charge of the film. This might enhance solubility and dissolution of shorter chain length or less cross-linked constituents in the polymeric matrix. If this is the case, the differences in cross-linking for polymerized $[Fe(4\text{-}CH_2Br\text{-}4'\text{-}CH_3bpy)_3]^{2+}$, where there are three polymerizable groups, and polymerized $[Fe(4,4'\text{-}(CH_2Br)_2bpy)_3]^{2+}$, where there are six, could explain the apparent difference in stability.

Synthetically, it would be useful to be able to prepare polymeric films where only one chelating ligand is required so that the contents of the other coordination sites could be varied at will. The preparation of films from $[Ru(bpy)_2(4,4'\text{-}(CH_2Br)_2bpy)]^{2+}$ was investigated with this goal in mind. In Figure 2A,B are shown cyclic voltammograms of solutions containing $[Ru(bpy)_2(4,4'\text{-}(CH_2Br)_2bpy)]^{2+}$ during formation of a film (A) and as the intact film in a fresh solution (B). The sharp oxidation peak on the return scan at −1.9 V has the appearance of a stripping peak. This provides evidence for adsorption of the monomer on the electrode

---

[11] Gould, S.; O'Toole, T. R.; Meyer, T. J. *J. Am. Chem. Soc.* **1990**, *112*, 9490.

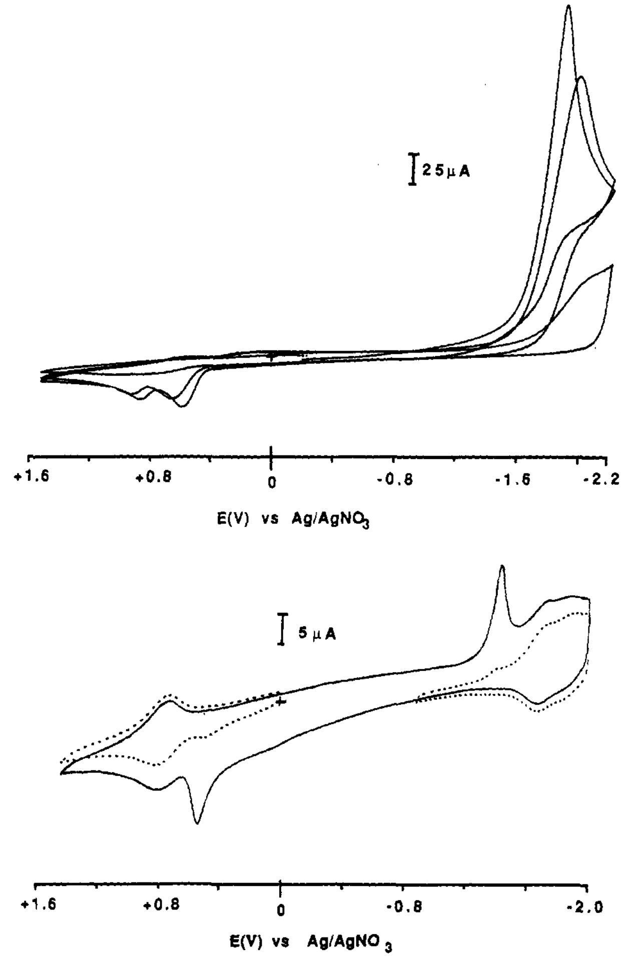

Figure 3. (A) Top: Cyclic voltammogram of a solution 3.7 mM in 4,4'-$(CH_2Br)_2$bpy, as in Figure 1. Scan rate = 100 mV/s. (B) Bottom: Cyclic voltammogram of a polymerized 4,4'-$(CH_2Br)_2$bpy film after soaking in an acetonitrile solution of $FeCl_2$ overnight. Scan rate = 100 mV/s.

when it is in the reduced state, an observation that has been made for twice-reduced $[Ru(bpy)_3]^{2+}$.[12] Electrochemical data are summarized in Table I.

Direct Polymerization of the Free Ligands. When electrodes immersed in solutions containing either 4,4'-$(CH_2Br)_2$bpy or 4-CH_2Br-4'-CH_3bpy were cycled repeatedly between +1.5 and −2.2 V, a metal-free film was deposited on the electrode surface. A cyclic voltammogram recorded during such an experiment based on 4,4'-$(CH_2Br)_2$bpy is shown in Figure 3A. As the film forms, the irreversible reduction at −1.9 V shifts to more negative potentials and decreases in magnitude upon subsequent scans. The irreversible peaks that appear at +0.57 and +0.84 V in an oxidative scan arise from the oxidation of Br^- to Br_2. The decrease in current and increase in overpotential for further reduction that occur with time are typical of electrode passivation. The rate at which passivation occurred was sensitive to the conditions used for the polymerization. When 0 V was used as the oxidative limit, the number of scans required to passivate the electrode was increased by factors of up to 2.

The ligand-based films remain on the electrode surface after rinsing with acetonitrile. They have no current response in cyclic voltammograms cycled between +1.4 and −2.0 V. When the films were soaked overnight in an acetonitrile solution containing 0.1 M $[N(n\text{-}Bu)_4](PF_6)$ and $FeCl_2$, an $Fe^{III/II}$ couple appeared at the same potential (+0.72 V) as in the films formed by electropolymerization of $[Fe(4,4'\text{-}(CH_2Br)_2bpy)_3]^{2+}$. The wave was somewhat broadened compared to the $Fe^{III/II}$ wave in those films.

Scheme I

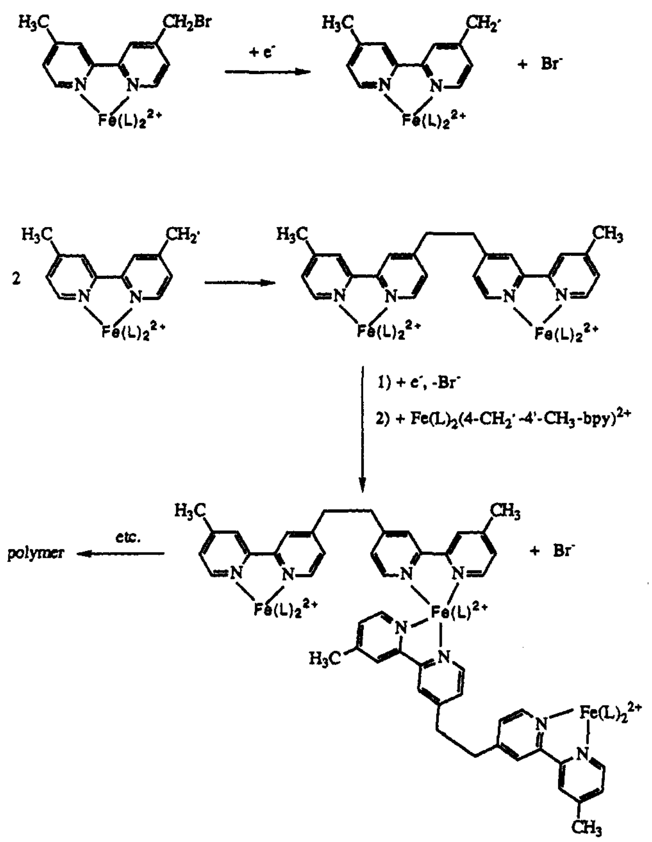

On the basis of the charge under the $Fe^{III/II}$ wave and with the assumption that 10^{-10} mol/cm^2 represents monolayer coverage, the coverage in Figure 3 was ~7.5 monolayers. This is a *lower* limit, since it assumes complete complexation of all bpy sites in the film.

Mechanism. There are several experimental facts that give insight into the mechanism of how the films are formed: (1) Polymerization is induced by an irreversible reduction. (2) During the polymerization, Br^- is released, as shown by the irreversible oxidation waves for Br^-. (3) The $E_{1/2}$ value for the $Fe^{III/II}$ couple shifts to more negative potentials. (4) From the spectroscopic and electrochemical properties of the films when compared to those of $[Fe(4,4'\text{-}(CH_3)_2\text{-}bpy)_3]^{2+}$, the integrity of the Fe^{II} complex remains essentially intact in the films.

From these observations and the known electrochemical behavior of haloaromatic compounds,[13] there are two likely mechanisms that would account for polymerization and formation of the films. They are illustrated in Schemes I and II by using $[Fe(4\text{-}CH_2Br\text{-}4'\text{-}CH_3bpy)_3]^{2+}$ as the example. In both cases, the initial step is dimerization. Subsequent reduction of a second 4-CH_2Br− group or of a 4-CH_2Br− group on a second ligand would eventually lead to polymeric chains and networks sufficiently long that insolubility-driven deposition occurs. As polymerized $[Fe(4\text{-}CH_2Br\text{-}4'\text{-}CH_3bpy)_3]^{2+}$ coats the electrode surface, further film growth relies on electron transfer from the electrode to the film/solution interface by electron-transfer hopping through intervening metal complex sites. In that sense, the film "mediates" electron transfer from the electrode to the solution.

Many of the observations that we have made can be explained by the model proposed here. From the broad, irreversible reduction wave in the initial scan in Figure 1A it can be inferred that reduction is followed by the rapid loss of Br^- and formation of polymer. The release of Br^- is shown by the appearance of the irreversible Br^- oxidation waves on initial oxidation scans and the

---

(12) Abruña, H. D.; Teng, A. Y.; Samuels, G. J.; Meyer, T. J. *J. Am. Chem. Soc.* **1979**, *101*, 6745.

(13) (a) M'Halla, F.; Pinson, J.; Saveant, J. M. *J. Electroanal. Chem. Interfacial Electrochem.* **1978**, *89*, 347. (b) Andrieux, C. P.; Blocman, C.; Dumas-Bouchiat, J.-M.; Saveant, J. M. *J. Am. Chem. Soc.* **1979**, *101*, 3431.

Scheme II

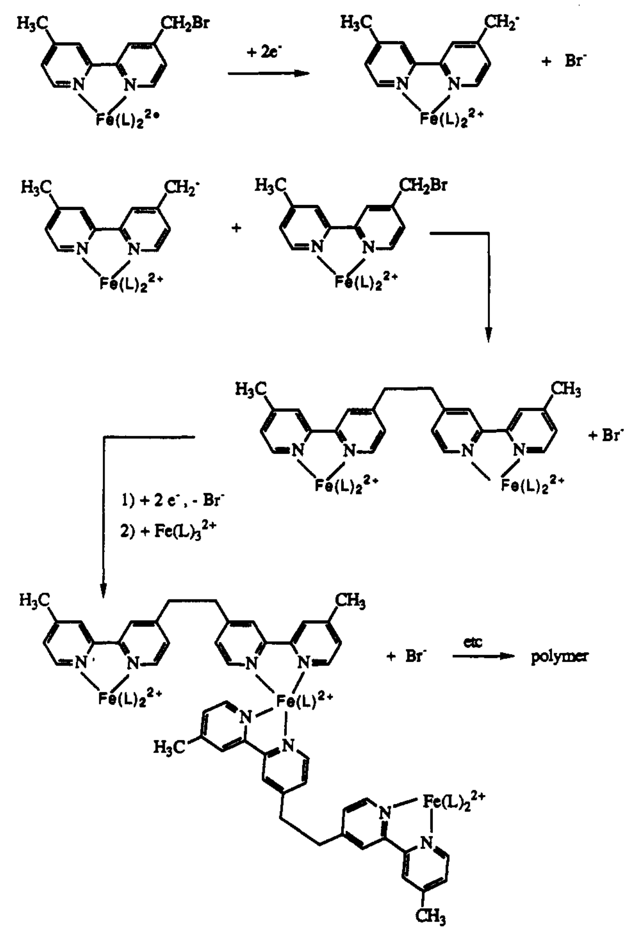

negative shift of the potential of the $Fe^{III/II}$ couple in the film. The appearance of the polymer on the electrode was shown by the appearance of the sharp prepeak in Figure 1A at −1.44 V. The origin of the prepeak may lie in the "mediated" reduction of $[Fe(4\text{-}CH_2Br\text{-}4'\text{-}CH_3bpy)_3]^{2+}$ in the external solution by the film. Since the complex in solution is blocked toward direct electron transfer from the electrode, its reduction cannot occur until the potential for the film-based couple at −1.74 V is approached. Electron-transfer mediation and the relative potentials of the film and solution-based couples play an important role in the continued growth of the films. For the films formed by electropolymerization of the free ligand, reduction at the π^* levels of the bpy sites in the poly(bipyridine) film occurred at a potential that was more negative than the limit used in the scans. At this more positive potential, mediated reduction does not occur. After several scans, the electrochemical activity ceased because the film acts as an insulator.

Polymerization of $[Zn(4\text{-}CH_2Br\text{-}4'\text{-}CH_3bpy)_3]^{2+}$ proceeded in much the same manner as for the Fe^{2+} complex, but the irreversible reduction, which initiated polymerization, can be resolved into components at −1.4, −1.54, and −1.68 V. There was no oxidative electrochemistry up to +1.4 V except for the appearance of the characteristic Br^- ion oxidation peaks in initial scans.

Previous work has shown that the Zn^{2+} ions in poly(bipyridyl) films are labile and can be removed by soaking films in solutions containing an appropriate chelating agent.[1e] If either or both of the coupling mechanisms presented in Schemes I and II are operative, the polymer formed upon electropolymerization of $[Zn(4\text{-}CH_2Br\text{-}4'\text{-}CH_3bpy)_3]^{2+}$ would consist of a 3-dimensional array of Zn^{2+} ions joined by bipyridine dimers. In this structure, the Zn^{2+} ions maintain the film structure by cross-linking. If they were removed, the structural integrity of the film should be lost and soluble bipyridyl fragments released to the solution.

Table II. Relative Rates of Polymerization[a]

	Γ, mol/cm²	Γ/Γ_0[b]
$[Ru(bpy)_2(vpy)_2]^{2+}$[c]	3.7×10^{-9}	1
$[Fe(4\text{-}CH_2Br\text{-}4'\text{-}CH_3bpy)_3]^{2+}$	5.8×10^{-9}	1.5
$[Fe(vbpy)_3]^{2+}$[c]	9.8×10^{-9}	3.1
$[Fe(4,4'\text{-}(CH_2Br)_2bpy)_3]^{2+}$	2.4×10^{-8}	7.3
$[Ru(bpy)_2(4,4'\text{-}(CH_2Br)_2bpy)]^{2+}$	1.8×10^{-10}	0.05

[a] Polymerizations were carried out by scanning the potential seven times from 0 to −2.0 V vs $Ag/AgNO_3$ at 100 mV/s. The solutions were 0.45–0.53 mM in 0.1 M $[N(n\text{-}Bu)_4](PF_6)$/acetonitrile. [b] Normalized for differences in the concentrations of the monomer in the electropolymerization solution by assuming that a linear relationship exists between surface coverage and monomer concentration. [c] vpy is 4-vinylpyridine; vbpy is 4-methyl-4′-vinyl-2,2′-bipyridine.

Relatively thick films of polymerized $[Zn(4\text{-}CH_2Br\text{-}4'\text{-}CH_3bpy)_3]^{2+}$ were grown on Pt screen and flag electrodes. They were soaked in an aqueous solution of Na_2S in order to remove Zn^{2+} as ZnS. After several hours, the electrodes were removed and rinsed with CH_2Cl_2. The soak/rinse cycle was repeated after which the aqueous and CH_2Cl_2 solutions were combined and extracted with fresh CH_2Cl_2. A visible coating remained on the electrode following this procedure. The CH_2Cl_2 fraction was reduced to dryness and the residue dried under vacuum. The proton NMR spectrum of the residue dissolved in $CDCl_3$ was consistent with a mixture of 4,4′-dimethyl-2,2′-bipyridine and the known dimeric bipyridine 1,2-bis[4-(4′-methyl-2,2-bipyridylyl)]ethane.[14] NMR (δ (ppm), ($CDCl_3$)): 2.4 (s, 7.6 H), 3.1 (s, 4 H), 7.1 (m, 4.9 H), 8.2 (s, 2.1 H), 8.3 (s, 2.0 H), 8.5 (d, 5 Hz, 2.2 H), 8.6 (d, 5 Hz, 2.2 H).

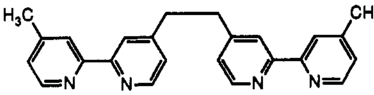

bpy dimer

In the ¹H NMR spectrum the ratio of $-CH_3$ to $-CH_2CH_2-$ protons was 7.6:4 while the ratio for the bpy dimer is 6:4. The appearance of 4,4′-dimethyl-2,2′-bipyridine as a product can be understood by assuming that a fraction of the radicals created by electrochemical reduction in Scheme I abstract a hydrogen atom from the solvent or the electrolyte in competition with radical–radical coupling.

In a related experiment, Fe^{2+} was removed from polymerized $[Fe(4\text{-}CH_2Br\text{-}4'\text{-}CH_3bpy)_3]^{2+}$. The films were prepared on Pt-gauze electrodes and removed by dissolution in concentrated HCl. The initial, pink solution underwent a rapid color change to pale yellow. To this solution was added an excess of Ce^{IV} and $EDTA^-$. The pH of the solution was raised to ~11 by adding aqueous KOH, and it was extracted with CH_2Cl_2. The CH_2Cl_2 extract was dried over Na_2CO_3 and subjected to thin-layer chromatography on alumina with 9:1 CH_2Cl_2/acetone as the eluent. The eluent contained 4,4′-dimethyl-2,2′-bipyridine (R_f = 0.86), the bpy dimer (R_f = 0.69), and at least one additional bipyridyl-containing product (R_f = 0.21).

Although C–C coupling is involved in the electropolymerization reaction, it can be inferred by the appearance of additional organic products that other coupling pathways contribute as well. This conclusion is consistent with the observation that the $4\text{-}CH_2Br\text{-}4'\text{-}CH_3bpy$ ligand itself forms polymeric films upon reduction, since, in this case, there is only a single polymerizable $4\text{-}CH_2Br-$ group. One possibility as a competing reaction is the ring-attack mechanism proposed by Guarr and Anson in the electropolymerization of $[Ru(vbpy)(L)_2]^{2+}$ (L is 1,10-phenanthroline or a related derivative).[15] When $[Ru(bpy)_3]^{2+}$ was added to a solution containing $4\text{-}CH_2Br\text{-}4'\text{-}CH_3bpy$ under the conditions used for electropolymerization, cyclic voltammetric measurements showed that the complex had been incorporated into the film. Under these conditions, $[Ru(bpy)_3]^{2+}$ does not undergo electropolymerization.

---

(14) Elliott, C. M.; Freitag, R. A.; Blaney, D. D. *J. Am. Chem. Soc.* **1985**, *107*, 4647.

(15) Guarr, T. F.; Anson, F. C. *J. Phys. Chem.* **1987**, *91*, 4037.

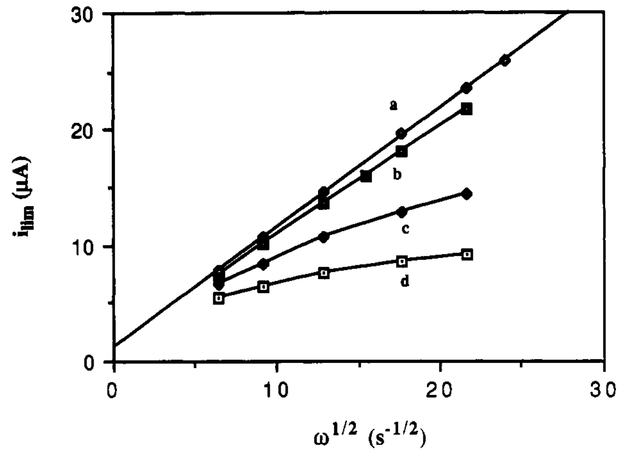

Figure 4. Levich plots of i_{lim} vs $\omega^{1/2}$ for the oxidation of ferrocene at a rotated-disk electrode. Curves a–d correspond to the response at (a) a bare Pt electrode (0.125 cm^2), (b) polymerized $[Fe(4\text{-}CH_2Br\text{-}4'\text{-}CH_3bpy)_3]^{2+}$ (Γ = 1.2 mol/cm^2), (c) polymerized $[Fe(4,4'\text{-}(CH_2Br)_2bpy)_3]^{2+}$ (Γ = 1.4 mol/cm^2), and (d) polymerized $[Fe(vbpy)_3]^{2+}$ (Γ = 0.92 mol/cm^2). The solution was acetonitrile 0.068 mM in ferrocene and 0.1 M in $[NEt_4](ClO_4)$. The scan rate was 20 mV/s.

Properties of the Films. Rates of Polymerization. Relative rates of electropolymerization, defined as Γ/Γ_0, the ratio of the surface coverage compared to the surface coverage for $[Ru(bpy)_2(vpy)_2]^{2+}$ obtained under the same conditions, are summarized in Table II. From the data, the rate of polymerization of $[Fe(vbpy)_3]^{2+}$ (vbpy is 4-methyl-4′-vinyl-2,2′-bipyridine) is bracketed by those for $[Fe(4\text{-}CH_2Br\text{-}4'\text{-}CH_3bpy)_3]^{2+}$ and $[Fe(4,4'\text{-}(CH_2Br)_2bpy)_3]^{2+}$. By inference, the vinyl polymerization is intrinsically more efficient toward film formation. The tris complex of $4,4'\text{-}(CH_2Br)_2bpy$ is even more efficient possibly because of the more favorable coupling statistics arising from the presence of the additional, polymerizable sites.

Molar Film Densities. Molar concentrations of redox sites within the films were calculated from surface coverages, Γ in mol/cm^2, and film thicknesses, *d*. They are related to the molar density by the relation, $C(\mathrm{M}) = \Gamma(\mathrm{mol/cm^2})/d(\mathrm{cm})$. Film thicknesses were measured by profilometry, and surface coverages, by integration of the charge passed during an oxidative or reductive voltammetric sweep. In order to have a flat surface for the film thickness measurements, the experiments were conducted on silicon wafers that had been coated with Pt. Apiezon wax evaporatively cast from CH_2Cl_2 or cyclohexane was used to mask off all but a small ~0.04-cm^2 square. Thin films (500–1000 Å) of the metallopolymer were deposited by cycling the electrode from +0.9 to −2.0 V at 50 mV/s. The Apiezon wax was removed by dissolution in CH_2Cl_2, and the surface coverage and film thicknesses were measured after drying. From these measurements the following molar densities were obtained: polymerized $[Fe(vbpy)_3]^{2+}$ (1.26 M), polymerized $[Fe(4\text{-}CH_2Br\text{-}4'\text{-}CH_3bpy)_3]^{2+}$ (0.93 M), and polymerized $[Fe(4,4'\text{-}(CH_2Br)_2bpy)_3]^{2+}$ (0.97 M). The value for polymerized $[Fe(vbpy)_3]^{2+}$ agreed with results obtained previously for polymerized $[Ru(vbpy)_3]^{2+}$.[16] From these results, it can be inferred that a more open, less dense structure exists in films prepared by the reduction of polypyridyl complexes containing the substituent $-CH_2Br$.

Permeation. The ability of ferrocene to diffuse through the polymeric films from the external solution to the electrode was investigated by rotating disk voltammetry. Experimentally, voltammetric curves were recorded at a series of rotation rates and the response was compared to those obtained at a bare, uncoated electrode. The voltammetric data were treated by using the inverse Levich–Koutecky equation in a form that describes the limiting current at a rotated disk electrode by assuming that mass transport through the films can be treated as a membrane diffusion process.[16,17]

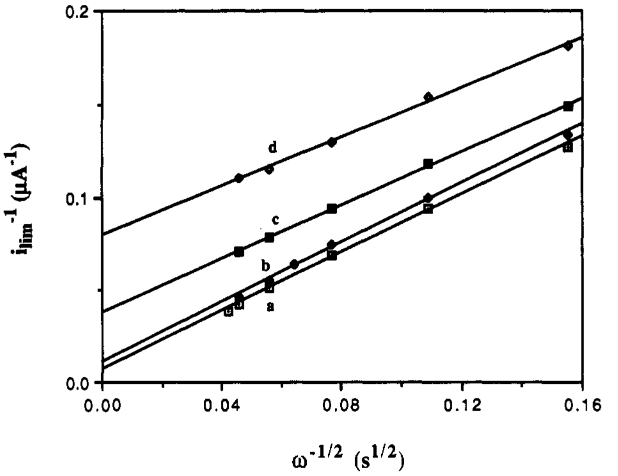

Figure 5. Koutecky–Levich plots of i_{lim}^{-1} vs $\omega^{-1/2}$ for the data presented in Figure 4 for the oxidation of ferrocene at (a) a bare Pt electrode, (b) polymerized $[Fe(4\text{-}CH_2Br\text{-}4'\text{-}CH_3bpy)_3]^{2+}$, (c) polymerized $[Fe(4,4'\text{-}(CH_2Br)_2bpy)_3]^{2+}$, and (d) polymerized $[Fe(vbpy)_3]^{2+}$.

Table III. Permeation of Ferrocene through the Films in 0.1 M $[N(Et)_4](ClO_4)/CH_3CN$ at Room Temperature

film	$10^9\Gamma$, mol/cm^2	10^3C_s, M	$10^8D_{s,pol}P$, cm^2/s	10^5D_s,[a] cm^2/s
polymerized $[Fe(vbpy)_3]^{2+}$	0.42	0.136	2.8	2.9
	0.67	0.075	2.5	2.9
	0.92	0.068	1.1	4.1
	1.09	0.075	1.2	4.5
polymerized $[Fe(4,4'\text{-}(CH_2Br)_2bpy)_3]^{2+}$	1.43	0.136	8.7	3.1
	1.44	0.068	4.8	3.6
	1.66	0.075	11.4	2.4
	2.16	0.075	4.9	3.3
	2.9	0.075	7.5	3.9
polymerized $[Fe(4\text{-}CH_2Br\text{-}4'\text{-}CH_3bpy)_3]^{2+}$	0.7	0.075	19.8	2.7
	0.73	0.136	10.3	3.2
	1.23	0.068	16.0	3.1
	1.37	0.075	22.9	3.3
	1.37	0.075	10.2	3.3
	2.18	0.075	32.4	3.0
	2.25	0.075	13.0	3.2
	2.24	0.075	25.6	3.2
	3.4	0.075	26.3	3.1

[a] Calculated from slopes of plots of i_{lim}^{-1} vs $\omega^{-1/2}$ by using 4.39 × 10^{-3} for ν. At the bare Pt electrode, $D_s = 2.4 \times 10^{-5}$ cm^2/s.

$$\frac{1}{i_{lim}} = \frac{1}{0.62nFAD_s^{2/3}\nu^{-1/6}\omega^{1/2}C_s} + \frac{1}{nFAD_{s,pol}PC_s/d}$$

n = number of electrons
F = Faraday constant
A = area of the electrode
$D_{s,pol}$ = diffusion coefficient for the electroactive species, S, within the film
P = partition coefficient of S between the film and the external solution
C_S = concentration of S in the solution
d = film thickness
D_S = diffusion coefficient for S in solution
ν = kinematic viscosity of the solvent
ω = rotation rate

In Figure 4 are shown typical Levich plots of i_{lim} vs $\omega^{1/2}$ for the oxidation of ferrocene at electrodes coated with polymerized $[Fe(4\text{-}CH_2Br\text{-}4'\text{-}CH_3bpy)_3]^{2+}$ ($\Gamma = 1.23 \times 10^{-9}$ mol/cm^2), $[Fe(4,4'\text{-}(CH_2Br)_2bpy)_3]^{2+}$ ($\Gamma = 1.44 \times 10^{-9}$ mol/cm^2), or $[Fe(vbpy)_3]^{2+}$ ($\Gamma = 0.92 \times 10^{-9}$). The response at the bare Pt electrode is included as a control. An inverse/inverse plot of i_{lim}^{-1} vs $\omega^{-1/2}$ for the data is shown in Figure 5. A value for the product

---

(16) (a) Ikeda, T.; Schmehl, R.; Denisevich, P.; Willman, K.; Murray, R. W. *J. Am. Chem. Soc.* **1982**, *104*, 2683. (b) Ewing, A. G.; Feldman, B. J.; Murray, R. W. *J. Phys. Chem.* **1985**, *89*, 1263.

(17) (a) Gough, D. A.; Leypoldt, J. K. *Anal. Chem.* **1979**, *51*, 439. (b) Leddy, J. A.; Bard, A. J. *J. Electroanal. Chem. Interfacial Electrochem.* **1983**, *153*, 223.

$D_{s,pol}\,P$ can be obtained from the y intercept.

The results of a series of such experiments are summarized in Table III. The quantity that can be derived from these plots that is of interest is the product of the diffusion coefficient through the film, $D_{s,pol}$, and the partition coefficient, P. For films of polymerized $[Fe(vbpy)_3]^{2+}$ values of $D_{s,pol}\,P$ were obtained that ranged from 1.1×10^{-8} to 2.8×10^{-8} cm²/s. These values are in good agreement with values obtained for the diffusion of ferrocene through polymerized $[Ru(vbpy)_3]^{2+}$.[16] From the data in Table III, the order of film permeabilities toward ferrocene increases as polymerized $[Fe(vbpy)_3]^{2+}$ < polymerized $[Fe(4,4'-(CH_2Br)_2bpy)_3]^{2+}$ < polymerized $[Fe(4-CH_2Br-4'-CH_3bpy)_3]^{2+}$. Films of polymerized $[Fe(4-CH_2Br-4'-CH_3bpy)_3]^{2+}$ were especially permeable toward the diffusion of ferrocene. Levich plots were linear within the range of available rotation rates.

The rates and the abilities of electroactive reagents to diffuse through the films depend upon the molecular volume of the permeant. For MnTPPCl (TPP is tetraphenylporphine), no current response for reduction was observed at polymerized $[Fe(4-CH_2Br-4'-CH_3bpy)_3]^{2+}$ ($\Gamma = 1.4 \times 10^{-9}$ to 3×10^{-9} mol/cm²). An oxidation wave for the $[Os(bpy)_2Cl_2]^{+/0}$ couple was observed, but the current levels were too small to analyze. For decamethylferrocene $D_{s,pol}P$ was found to be 5.2×10^{-9} cm²/s. On the basis of evidence in these data for size discrimination, we conclude that transport to the electrode through polymerized $[Fe(4-CH_2Br-4'-CH_3bpy)_3]^{2+}$ is not primarily through large channels or film imperfections.

The decreased permeability toward diffusion of ferrocene for polymerized $[Fe(4,4'-(CH_2Br)_2bpy)_3]^{2+}$ compared to polymerized $[Fe(4-CH_2Br-4'-CH_3bpy)_3]^{2+}$ is consistent with an increase in the average chain length or degree of cross-linking in the former due to the increased number of polymerizable sites on the ligand. The polymerized $[Fe(vbpy)_3]^{2+}$ films were the least permeable of the films studied consistent with its higher molar density. This result is somewhat surprising, since each ligand contains only one polymerizable site and the polymer must have a longer link between adjacent complexes. These films may be more highly cross-linked and less susceptible to swelling when exposed to solvent.

Preparation of Polymeric Films of Controlled Composition. Bilayers and Copolymers. The versatility of the electropolymerization procedure in the preparation of polymeric films of controlled composition and structure is well documented.[1a,b,18] Layered structures can be prepared by sequential electropolymerization. Films of varying chemical composition can be prepared by copolymerization of two or more components. We have conducted a series of experiments in which it was demonstrated that both layered structures and copolymeric films can be prepared by using the bromomethyl-derivatized bipyridine ligands. In addition, we have found that the polymerization of these complexes is completely compatible with those based on vbpy.

Copolymeric Films. Copolymerization of $[Fe(4,4'-(CH_2Br)_2bpy)_3]^{2+}$ and $[Ru(bpy)_2(4,4'-(CH_2Br)_2bpy)]^{2+}$. A copolymeric film containing polymerized $[Ru(bpy)_2(4,4'-(CH_2Br)_2bpy)]^{2+}$ and $[Fe(4,4'-(CH_2Br)_2bpy)_3]^{2+}$ was prepared by reductive electropolymerization. The solution used to prepare the films was 0.19 mM in $[Fe(4,4'-(CH_2Br)_2bpy)_3]^{2+}$ and 0.70 mM in $[Ru(bpy)_2(4,4'-(CH_2Br)_2bpy)]^{2+}$ (21:79 Fe^{2+}:Ru^{2+}). The cyclic voltammetric response obtained from the copolymeric film is shown in Figure 6A. Waves for the $Ru^{III/II}$ and $Fe^{III/II}$ couples were observed at +0.96 and +0.70 V, respectively. On the basis of the integrated waveforms, the ratio of Fe^{2+} to Ru^{2+} was 26:74 in the film.

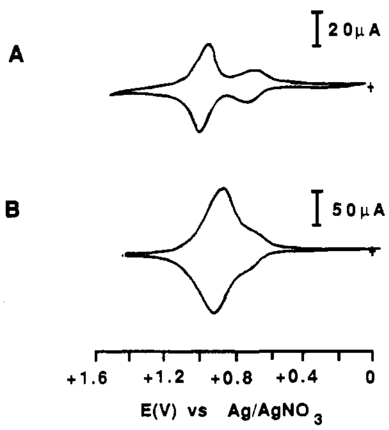

Figure 6. (A) Cyclic voltammogram of a copolymeric film consisting of polymerized $[Fe(4,4'-(CH_2Br)_2bpy)_3]^{2+}$ and $[Ru(bpy)_2(4,4'-(CH_2Br)_2bpy)]^{2+}$ in acetonitrile that was 0.1 M in $[N(n-Bu)_4](PF_6)$. The scan rate was 100 mV/s. (B) Cyclic voltammogram of a copolymeric film of polymerized $[Fe(4,4'-(CH_2Br)_2bpy)_3]^{2+}$ and $[Ru(vbpy)_3]^{2+}$, as in (A).

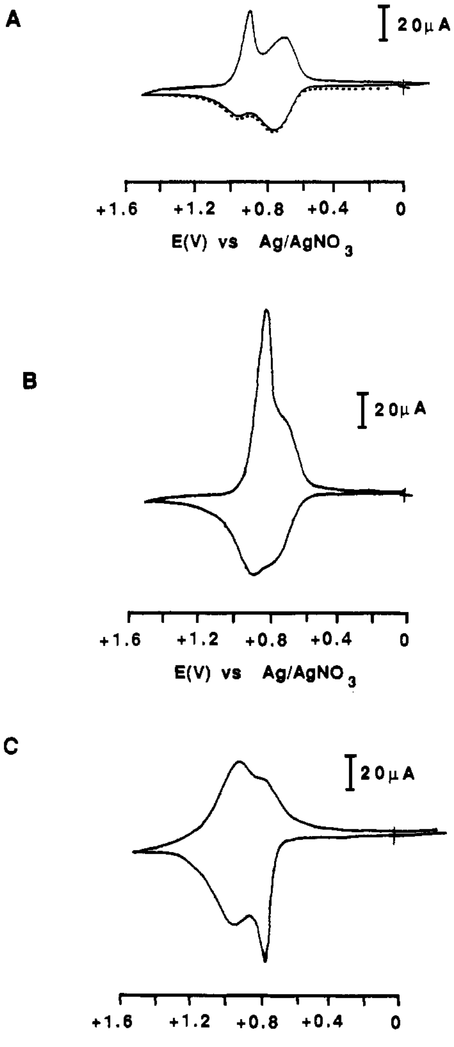

Figure 7. (A) Cyclic voltammogram of a bilayer structure consisting of $Pt/[Fe(4,4'-(CH_2Br)_2bpy)_3]^{2+}/[Ru(bpy)_2(4,4'-(CH_2Br)_2bpy)]^{2+}$ in acetonitrile that was 0.1 M in $[N(n-Bu)_4](PF_6)$. Scan rate = 100 mV/s. (B) Cyclic voltammogram of $Pt/[Fe(4,4'-(CH_2Br)_2bpy)_3]^{2+}/[Ru(vbpy)_3]^{2+}$, as in (A). (C) Cyclic voltammogram of $Pt/[Ru(vbpy)_3]^{2+}/[Fe(4,4'-(CH_2Br)_2bpy)_3]^{2+}$, as in (A).

Copolymerization of $[Fe(4,4'-(CH_2Br)_2bpy)_3]^{2+}$ and $[Ru(vbpy)_3]^{2+}$. In a related experiment, a copolymer of polymerized $[Fe(4,4'-(CH_2Br)_2bpy)_3]^{2+}$ and $[Ru(vbpy)_3]^{2+}$ was prepared by the electropolymerization of a solution that was 0.19 mM in $[Fe(4,4'-(CH_2Br)_2bpy)_3]^{2+}$ and 0.41 mM in $[Ru(vbpy)_3]^{2+}$ (37:69 Fe^{2+}:Ru^{2+}). A cyclic voltammogram for the resulting film is shown

---

[18] (a) Denisevich, P.; Willman, K. W.; Murray, R. W. *J. Am. Chem. Soc.* **1981**, *103*, 4727. (b) Willman, K.; Murray, R. W. *J. Electroanal. Chem. Interfacial Electrochem.* **1982**, *133*, 211. (c) Pickup, P. G.; Leidner, C. R.; Denisevich, P.; Murray, R. W. *J. Electroanal. Chem. Interfacial Electrochem.* **1984**, *164*, 39. (d) Downard, A. J.; Surridge, N. A.; Cosnier, S.; Deronzier, A.; Moutet, J.-C.; Meyer, T. J. *J. Electroanal. Chem. Interfacial Electrochem.* **1988**, *246*, 321.

in Figure 6B. The presence of both couples in the film is evidenced by the waves that appear at +0.88 and +0.70 V corresponding to the Ru$^{III/II}$ and Fe$^{III/II}$ couples, respectively. By integration, the ratio of Fe^{2+} to Ru^{2+} in the copolymeric film was 16:84.

Copolymerization of [Ru(bpy)$_2$(4,4′-(CH$_2$Br)$_2$bpy)]$^{2+}$ and [Os(vbpy)$_3$]$^{2+}$. A solution 1.08 M in [Ru(bpy)$_2$(4,4′-(CH$_2$Br)$_2$bpy)$^{2+}$ and 0.73 M in [Os(vbpy)$_3$]$^{2+}$ (60:40 Ru^{II}:Os^{II}) was electropolymerized by scanning the potential to −1.4 V. At this potential only the Ru^{2+} complex was reduced. This experiment was conducted to see if copolymerization could be induced by selective reduction at the Ru^{2+} complex. In the cyclic voltammogram of the resulting film reversible waves appeared at +0.41 and +1.00 V for the Os$^{III/II}$ and Ru$^{III/II}$ couples, respectively. By integration, the ratio of Ru^{II} to Os^{II} was 73:27. In a control experiment in which there was only [Os(vbpy)$_3$]$^{2+}$ in the polymerization solution, no significant electropolymerization was observed.

Layered Structures. In order to facilitate this part of the presentation, layered structures will be represented in the format: electrode/component 1/component 2. In this representation component 1 is the initially electropolymerized monomer. After electropolymerization, it is at the electrode/film interface. Component 2 is the monomer that was electropolymerized as a second film, atop the first, in a second step. After the second electropolymerization it is at the film/solution interface.

Pt/[Fe(4,4′-(CH$_2$Br)$_2$bpy)$_3$]$^{2+}$/[Ru(bpy)$_2$(4,4′-(CH$_2$Br)$_2$bpy)]$^{2+}$. The preparation of an inner layer of electropolymerized [Fe(4,4′-(CH$_2$Br)$_2$bpy)$_3$]$^{2+}$ ($\Gamma = 5.4 \times 10^{-9}$ mol/cm^2) was carried out initially. This step was followed by the electropolymerization of [Ru(bpy)$_2$(4,4′-(CH$_2$Br)$_2$bpy)]$^{2+}$ in a second step. A cyclic voltammogram for the resulting "bilayer" is shown in Figure 7A. In the voltammogram, waves for both the Ru$^{III/II}$ and Fe$^{III/II}$ couples were observed. The reductive component for the Ru$^{III/II}$ wave appeared as a sharp prepeak at the onset of the reductive component for the Fe$^{III/II}$ wave. This is due to an enhancement in the rate of reduction of the Ru^{3+} in the outer layer. At the onset of reduction of Fe^{3+} in the inner layer, the Fe^{2+} produced can, in turn, reduce Ru^{3+}, which is spatially isolated in the outer layer. Thus, reduction of Ru^{3+} is mediated by Fe^{2+}. This behavior is in contrast to the copolymeric film in Figure 6A where neither of the component waves is distorted. Both components are in the inner layer and have direct channels for undergoing electron transfer with the electrode surface.

Pt/[Fe(4,4′-(CH$_2$Br)$_2$bpy)$_3$]$^{2+}$/[Ru(vbpy)$_3$]$^{2+}$. An inner layer of electropolymerized [Fe(4,4′-(CH$_2$Br)$_2$bpy)$_3$]$^{2+}$ ($\Gamma = 7.8 \times 10^{-9}$ mol/cm^2) was prepared on a Pt electrode. In a second electropolymerization step an outer layer of polymerized [Ru(vbpy)$_3$]$^{2+}$ was added. A cyclic voltammogram of the resulting film is shown in Figure 7B. The overlap between the Ru$^{III/II}$ and Fe$^{III/II}$ waves is greater than in the previous case. A sharp prepeak is still observed at the onset of the Fe$^{III/II}$ reduction due to the mediated reduction of Ru^{3+} in the outer layer by Fe^{2+} in the inner layer.

Pt/[Ru(vbpy)$_3$]$^{2+}$/[Fe(4,4′-(CH$_2$Br)$_2$bpy)$_3$]$^{2+}$. A layer of polymerized [Ru(vbpy)$_3$]$^{2+}$ ($\Gamma = 7.6 \times 10^{-9}$ mol/cm^2) was formed by reductive electropolymerization. In a second step a layer of electropolymerized [Fe(4,4′-(CH$_2$Br)$_2$bpy)$_3$]$^{2+}$ was added. In Figure 7C is shown a cyclic voltammogram of the resulting bilayer film. The sharp prepeak observed at the onset of the oxidative component for the Ru$^{III/II}$ couple is a consequence of the bilayer structure. The outer layer, which contains Fe^{2+}, is isolated from the electrode. Oxidation of Fe^{2+} requires mediation by the Ru^{3+} sites in the inner layer. Reductive components for both the Ru$^{III/II}$ and Fe$^{III/II}$ couples are observed on the return scan. The reduction of Fe^{3+} to Fe^{2+} occurs because of the large overlap between the Ru$^{III/II}$ and Fe$^{III/II}$ waves.[18a] Fe^{3+} in the outer layer formed in the oxidative scan cannot be trapped.

Acknowledgment is made to the Army Research Office under Grant No. DAAL03-90-G-0062 for support of this work and to Kimberly Hooker for providing the XPS results. XPS instrumentation was funded by an instrumentation grant (R. W. Linton, Principal Investigator) from the Office of Naval Research, ONR No. N00014-86-G-0200.

Notes

Contribution from the Science and Engineering Research
Laboratory, Waseda University, Ohkubo 3-4-1,
Shinjuku-ku, Tokyo 169, Japan

Photochemistry of Chlorochromium(III) Tetraphenylporphyrinate in Acetone. Studies on Photodissociation of the Axial Acetone in the Temperature Range 180–295 K by Laser Photolysis

Minoru Yamaji†

Received August 15, 1990

It is well-known that natural and synthetic metalloporphyrins undergo photodissociation of the axial ligand such as CO, NO, O$_2$, CN$^-$, or pyridine upon light irradiation. By means of pico- and nanosecond laser photolyses, many studies of the reactive state for the ligand dissociation as well as on deactivation processes of excited states have been carried out.[1] These studies help extensively to understand the effects of the axial ligand on the excited-state behavior of metalloporphyrins.

For chromium porphyrins, in our previous paper,[2] it was reported that the pyridinate of ClCr^{III}(TPP), ClCr^{III}(TPP)Py (Py = pyridine), in acetone photodissociates the axial pyridine to produce ClCr^{III}(TPP) with a quantum yield of 0.16 upon both 355- and 532-nm laser irradiation at room temperature. Since no excitation wavelength dependence was observed, we had three candidates for the reactive state for dissociation: the triplet–sextet, ^{6}T$_1$, the triplet–quartet, ^{4}T$_1$, and the singlet–quartet, ^{4}S$_1$, states.[3] On the basis of the following two reasons, neither the ^{4}T$_1$ nor the ^{6}T$_1$ state is the reactive state: (1) the quantum yields for photodissociation are independent of the concentrations of oxygen; (2) the ^{6}T$_1$ state, which is in thermal equilibrium with the ^{4}T$_1$ state, is quenched by oxygen. Therefore, the ^{4}S$_1$ state wsa concluded to be the reactive state for the dissociation of Py from ClCr^{III}(TPP)Py.

In the present work, we have investigated the photochemistry of the photodissociation of the axial acetone from the acetonate of ClCr^{III}(TPP), ClCr^{III}(TPP)Ac (Ac = acetone), by laser pho-

---

† Present address: Department of Chemistry, Faculty of Engineering, Gunma University, Kiryu, Gunma 376, Japan.

(1) (a) Lavalette, D.; Tetreau, C.; Momenteau, M. *J. Am. Chem. Soc.* **1979**, *101*, 5395–5401. (b) Hoshino, M.; Kashiwagi, Y. *J. Phys. Chem.* **1990**, *94*, 673–678. (c) Hoshino, M. *Chem. Phys. Lett.* **1985**, *120*, 50–52. (d) Hoffman, B. M.; Gibson, Q. H. *Proc. Natl. Acad. Sci. U.S.A.* **1978**, *75*, 21–25. (e) Hoshino, M.; Arai, S.; Yamaji, M.; Hama, Y. *J. Phys. Chem.* **1985**, *90*, 2109–2111. (f) Tait, C. D.; Holten, D.; Gouterman, M. *J. Am. Chem. Soc.* **1984**, *106*, 6653–6659. (g) Hoshino, M.; Kogure, M.; Amano, K.; Hinohara, T. *J. Phys. Chem.* **1989**, *93*, 6655–6659.

(2) Yamaji, M.; Hama, Y.; Hoshino, M. *Chem. Phys. Lett.* **1990**, *165*, 309–314.

(3) Gouterman, M.; Hanson, L. K.; Khalil, G.-E.; Leenstra, W. R.; Buchler, J. W. *J. Chem. Phys.* **1975**, *62*, 2343–2353.

0020-1669/91/1330-2949$02.50/0